Available online at www.sciencedirect.com
SCIENCE DIRECT
Polymer 46 (2005) 6614–6622
polymer
www.elsevier.com/locate/polymer

Interactions and mechanical properties of rod–coil ionomer blend

Andreas Bayer, Achim Datko, Claus D. Eisenbach*

Institut für Angewandte Makromolekulare Chemie, Universität Stuttgart, Pfaffenwaldring 55, D-70569 Stuttgart, Germany

Available online 26 May 2005

Abstract

Polymer–polymer blends of rigid-rod and random-coil macromolecules are obtained by ionomer blend formation. The molecular dispersion of the rod molecules in the matrix polymer is achieved by acid–base interactions. The reinforcement effect in terms of the Young's modulus is discussed as a function of the degree of polymerization of the rods. By treating the reinforcer molecule as a fuzzy cylinder the reinforcement effect can be correlated to the reinforcers' size and shape.

Keywords: Ionomer blends; Molecular reinforcement; Nanocomposites

1. Introduction

Rod–coil polymer polymer blends are interesting since they represent the molecular extreme of a classical fiber composite material. If both components form a one phase system, such blends are expected to be superior to conventionally reinforced materials like glass- or carbon-fiber filled plastics [1–4]: as a consequence of the atomic scale diameter of the rod-like molecules and the associated high aspect ratio, ultimate reinforcement effects have been predicted for rigid-rod polymer composites [1,3]; besides, problems known for macroscopic fiber reinforced materials, e.g. limited fiber-matrix adhesion and different thermal expansion coefficients of fiber and matrix polymer are not relevant for a molecular polymer/polymer composite.

However, a serious obstacle for achieving the ideal of such a molecular composite (Fig. 1(a)) is the fact that most polymers are immiscible due to the unfavorable entropy of mixing. This applies particularly to mixtures of rod- and coil-like polymer components [5] which typically form phase separated systems: the rod molecules tend to segregate and to form domains in the matrix phase of the coiled polymer component as shown in Fig. 1(b). Thus, to overcome this entropy-driven demixing, attractive forces between the polymer components need to be introduced to generate a sufficiently negative enthalpy of mixing [6–10].

Similarly, as has been shown for mixtures of random coil polymers that homogeneous blends can be obtained by, e.g. hydrogen bondings [11,12], charge-transfer complexes [13], or ionic interactions [14], especially the latter ones were proven to be suited for mixing comparatively stiff liquid crystalline polymers with flexible coiled matrix polymers [15,16]. Strong ionic interactions are also the key for the formation of homogeneous blends consisting of rod-like polymer chains molecularly dispersed in the coil polymer matrix [17–24]. Theoretical considerations [25] starting from the original Flory theory [5] confirmed the experimental results of molecular ionomer blends which are based on a sufficiently negative rod–coil interaction parameter.

This paper will focus on ionomer blends with cation/anion interactions formed in situ by mixing acidic rod-like and basic coil macromolecules: sulfonated poly(*para*-phenylene) with alkyl side chains (PPPSH) represents the reinforcer component, and poly(ethyl acrylate-*co*-4-vinyl pyridine) P(EA-*co*-4VP) or poly(styrene-*co*-4-vinyl pyridine) P(S-*co*-4VP) have been employed as matrix material (Fig. 2). The features of molecular miscibility will be presented and the molecular parameters of the reinforcing rod-like polymer chains which determine the mechanical properties of the acid/base ionomer blend will be discussed.

* Corresponding author. Tel.: +49 711 685 4440; fax: +49 711 685 4396.
E-mail address: cde@makro.chemie.uni-stuttgart.de (C.D. Eisenbach).

0032-3861/$ - see front matter © 2005 Elsevier Ltd. All rights reserved.
doi:10.1016/j.polymer.2005.05.015

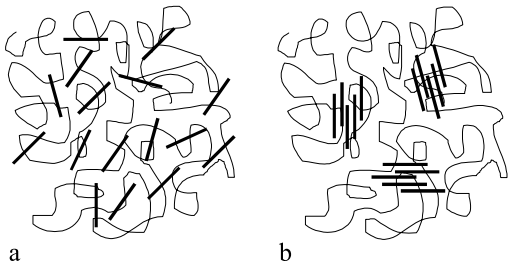

Fig. 1. Schematic of the morphology of a rigid-rod/flexible coil polymer blend: (a) molecularly dispersed mixture and (b) microphase separated system with segregated rigid rods.

2. Experimental part

2.1. Materials

PPPSH of different number average degree of polymerization P_n was synthesized as described elsewhere [26–28]. The matrix polymers P(EA-*co*-4VP) and P(S-*co*-4VP) (8 mol% 4VP) were synthesized by free radical copolymerization of ethyl acrylate (EA) or styrene (S) and 4-vinyl pyridine (4VP) in bulk (0.2 mol% AIBN as initiator; 65 or 50 °C, respectively); molecular weights $M_n = 200.000$ and 190.000, respectively, ($M_w/M_n = 2$).

2.2. Polymer characterization

The composition of the matrix polymer was determined by NMR-spectroscopy and titration. The molecular weights were obtained by gel permeation chromatography (GPC). Polystyrene calibration was employed for the matrix polymer analysis; the P_n of the rod-like PPPSH is based on the analysis of the poly(*p*-phenylene sulfonic acid ester) precursor molecules (PPPSE) by using the correct PPPSE calibration curve [28]. The glass transition temperatures T_g were determined by DSC analysis (see below).

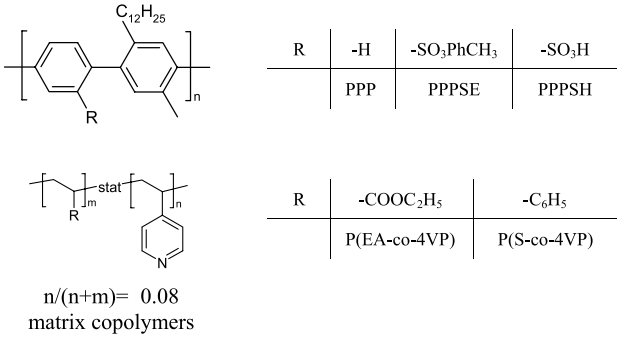

Fig. 2. Chemical structures of poly(*p*-phenylene) type rod-like molecules and vinyl pyridine (VP) matrix copolymers, and schematic of the acid/base ion pair in the ionomer blends of sulfonated poly(*p*-phenylene) PPPSH and VP copolymers.

2.3. Blend formation

The rod–coil ionomer blends were prepared by simultaneously dropping separate THF solutions of the two blend components (0.2–1 wt%, stoichiometry of acidic/basic groups) into the cosolvent THF. The resulting gel phase was isolated and dried. To estimate possible solvent effects, one ionomer blend sample was prepared from $CHCl_3$ solution (see below). Test specimens were obtained by compression molding of the coprecipitate: (P(EA-*co*-4VP)-based blends: 170 °C/10–15 kN; P(S-*co*-4VP)-based blends: 200 °C/10–15 kN).

2.4. Blend characterization

IR spectroscopy was performed with a Bruker IFS 66/S FTIR instrument equipped with a single-reflex ATR-unit. DSC measurements were conducted with a Perkin–Elmer Pyris 1 instrument and a heating rate of 20 K/min. Stress–strain measurements (strain rate 5 mm/min) were performed with an Instron 4301 system equipped with a temperature-controlled unit at ambient temperature (EA copolymer matrix) and 150 °C (S copolymer matrix); dimensions of the samples were $10 \times 2.8–3.3 \times 0.4–0.7$ mm^3 (EA copolymer matrix) and $5 \times 2.8–3.3 \times 0.4–0.7$ mm^3 (S copolymer matrix, length × width × thickness).

3. Results and discussion

3.1. Molecular miscibility in blend formation

As already discussed above, one successful approach to generate molecular blends of rod-like and coil molecules is to introduce ionic interactions between the blend components. In the present case, this is realized by proton transfer from PPPSH to the basic matrix polymer resulting in a sulfonate–pyridinium ion pair as schematically shown in Fig. 2. This can be monitored from the IR analysis of the pyridine ring vibrations band [29]. The pure matrix material P(EA-*co*-4VP) shows signals of the unprotonated pyridine at 1600 and 1557 cm^{-1} as exemplarily seen for P(EA-*co*-4VP) ((1) in Fig. 3); the pure reinforcing polyelectrolyte $PPPS^-Na^+$ does not exhibit any signal in this range of the spectra ((4) in Fig. 3). When the matrix polymer is blended with a stoichiometric amount of the reinforcing polymer PPPSH, the nearly complete disappearance of the pyridine

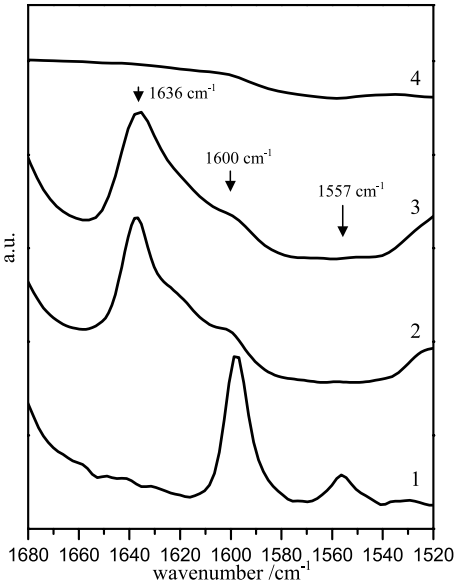

Fig. 3. IR-spectra (absorption) of the matrix polymer P(EA-*co*-4VP) (1), of the protonated P(EA-*co*-4VPH^+) model polyelectrolyte formed with *p*-toluene sulfonic acid (TsOH) (2), of the sodium sulfonate PPPS^-Na^+ of the reinforcer PPPSH (4), and of the acid/base ionomer blend P$PPS2^-$/P(EA-*co*-4VPH^+) (3) co-precipitated from THF solution (Table 1).

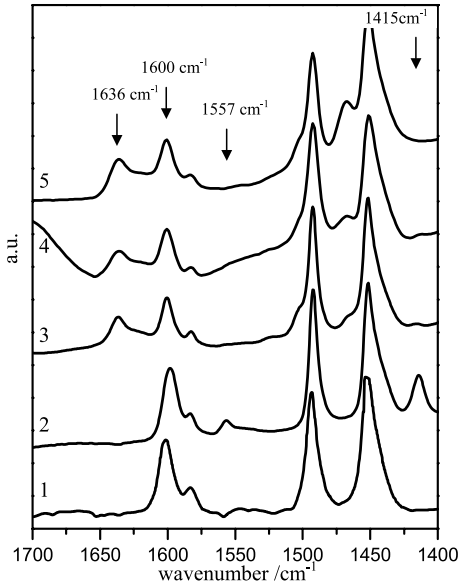

Fig. 4. IR-spectra (absorption) of polystyrene (1), of the matrix polymer P(S-*co*-4VP) (2), of the protonated P(S-*co*-4VPH^+) model polyelectrolyte formed with *p*-toluene sulfonic acid (TsOH) (3), and blends of PPPSH2 and P(S-*co*-4VP) (Table 1) as obtained by co-precipitation from THF (4) or $CHCl_3$ solution (5).

band and the appearance of a new band at 1636 cm^{-1} characteristic for the pyridinium ((3) in Fig. 3) indicate the extensive proton transfer from the sulfonic acid group of the PPPSH to the P(EA-*co*-4VP) matrix polymer; this is confirmed from the practically identical spectrum of the matrix polymer tosylate ((2) in Fig. 3).

In case of the blends with P(S-*co*-4VP), the disappearance of the 1600 cm^{-1} band cannot be used as proof for the protonation of the pyridinium moiety because the band of the phenyl group of the styrene comonomer is dominating in this region (compare (1) and (2) in Fig. 4). However, the decreasing pyridine bands at 1557 and 1415 cm^{-1} and the appearing of the pyridinium-typical signal at 1636 cm^{-1} indicate the acid/base ionomer blend formation (spectra 4 or 5 in comparison to spectrum 2, Fig. 4). As in the case of the P(EA-*co*-4VP) matrix blends, this band assignment is supported by the tosylate P(S-*co*-4VPH^+)TsO^- ((3) in Fig. 4). The blend spectrum is almost identical to that of this protonated model system P(S-*co*-4VPH^+)TsO^-. Thus, the ionomer formation has been verified and the miscibility of the rod with the coil macromolecules is also fulfilled for the polystyrene-based blends.

However, it shall be mentioned that the little residual band at about 1415 cm^{-1} in the spectra of both the tosylate ionomer (spectrum 3) and the ionomer blend (spectrum 4, Fig. 4) made with P(S-*co*-4VP) indicates a small amount of unprotonated pyridine groups which is not observed in the blends made with P(EA-*co*-4VP). In contrast to this finding for the P(S-*co*-4VP)-based blends as obtained from THF solvent, complete disappearance of the 1415 cm^{-1} band of these blends is observed when chloroform is employed instead of THF solvent ((5) in Fig. 4). This different behavior in the ionomer blend formation is explained by the basicity of the THF solvent and the vitrification of the PPPS^-/P(S-*co*-4VPH^+) blends during solvent evaporation: once the glass transition temperature T_g of the not yet completely solvent-free blend has exceeded the drying temperature, the mobility of the ionic species which include protonated THF does not allow for a quantitative protonation of the more basic pyridine moiety but partial reformation of sulfonic acid groups by proton transfer from THF occurs. This is not the case for the PPPS^-/P(EA-*co*-4VPH^+) blend formation where the T_g of the matrix polymer as well as of the ionomer blends always stays below the drying temperature (ambient temperature up to about 100 °C). If THF solvent is replaced by $CHCl_3$, the competitive protonation between pyridine moieties of the matrix polymer and (THF) solvent molecules is not given, and quantitative proton transfer is observed (spectrum 4 in comparison to spectrum 3, Fig. 4).

In summary, the proton exchange has been proven by IR spectroscopical analysis. This means that the attractive forces between the reinforcing component and the matrix materials which are a fundamental requirement of miscibility have been generated in both matrix polymer systems.

Further experimental evidence for the miscibility of the binary rod/coil system is given by DSC analysis (Figs. 5 and 6). The trace of the pure PPPSH and PPP indicates only weak transitions at about 70–90 °C (curves 4 and 5, Fig. 5) [28]. The matrix materials show well-defined glass

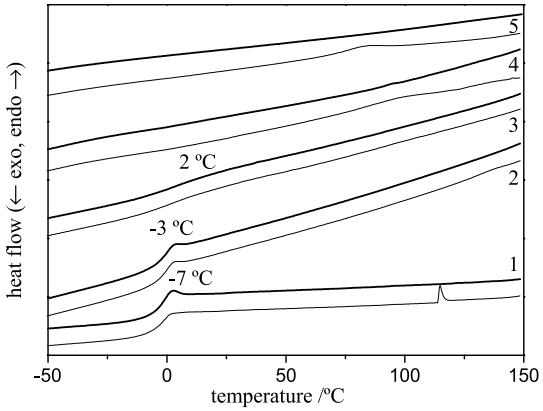

Fig. 5. DSC curves (thin curve: first heating run, bold curve: second heating run) of the (PEA-*co*-4VP) matrix polymer (1), of PPP (5) and the reinforcer polymer PPPSH3 (4), and of the ionomer blend $PPPS3^-/P(EA\text{-}co\text{-}4VPH^+)$ (curve 3; 25 wt% PPPSH and stoichiometry of acid/base groups) as well as of the PPP/P(EA-*co*-4VP) blend (curve 2). The arrows indicate the glass transition temperatures of the second heating runs.

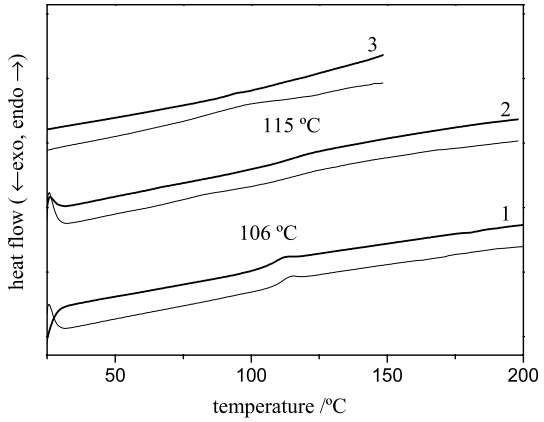

Fig. 6. DSC curves (thin curve: first heating run, bold curve: second heating run) of the (PS-*co*-4VP) matrix polymer (curve 1), of the reinforcer polymer PPPSH3 (curve 3), and of the ionomer blend $P(S\text{-}co\text{-}4VPH^+)/PPPS3^-$ (curve 2; 23 wt% PPPSH and stoichiometry of acid/base groups). The arrows indicate the glass transition temperatures of the second heating runs.

transition temperatures (T_g) at about −7 °C (P(EA-*co*-4VP), (1) in Fig. 5) and 106 °C (P(S-*co*-4VP), (1) in Fig. 6), respectively. The DSC trace of the blend of the matrix polymer P(EA-*co*-4VP) with the poly(*p*-phenylene) PPP not carrying the acidic functional (sulfonic) groups showed the same relatively sharp α-transition characteristic of the matrix polymer at only little higher temperature (curve 1 and 2, Fig. 5); this is indicative of a phase separated blend as schematically shown in Fig. 1(b).

In contrast to this, the DSC traces of the stoichiometric acid/base $PPPS^-/P(EA\text{-}co\text{-}4VPH^+)$ blend resulting from mixing of the reinforcing polymer and matrix polymer carrying complementary ionizable groups showed a relatively broad single glass transition which is shifted about 8–13 K towards higher temperatures as compared to the matrix (Table 1); as for this particular example represented in Fig. 5, T_g is about 2 °C (curve 3 in Fig. 5). Phenomenologically similar features as seen for the P(EA-*co*-4VP)-based blends (Fig. 5) were also observed with P(S-*co*-4VP) matrix, but—as a consequence of the much higher T_g of the pure matrix polymer—in a significantly higher temperature regime (Fig. 6). Such a single and relatively broad glass transition temperature regime observed at higher temperature than the T_g of the corresponding matrix polymer [28] has also been observed for the other rod/coil ionomer blends [23,25]; this is indicative of both the miscibility of the blend components and the multiple ionic interactions along the one-dimensional rod, respectively.

If we postulate that the glass transitions observed in the ionomer blends are solely correlated to main chain motions of the matrix molecules, which is reasonable regarding the low weight fraction and the rigidity of the reinforcing molecules, the T_g shift towards higher temperatures can be understood on a molecular level: any anion/cation pair formed between the multiple anionic reinforcer polyelectrolyte and a matrix cation acts like a crosslink. This means that matrix polycation segments are immobilized along the reinforcer backbone. This view is meaningful if taking into account the long-distance interactions of ionic groups and the high charge density along the sulfonated rod-like

Table 1
Molecular characteristics of the PPPSH reinforcer polymer samples (average degree of polymerization P_n and contour length L_K) and thermal (glass transition temperature T_g) as well as mechanical properties (Young's modulus E_Y) of the blends with P(EA-*co*-4VP) and P(S-*co*-4VP)

Reinforcer	PPPSH1	PPPSH2	PPPSH3	PPPSH4	PPPSH5	PPPSH6	PPPSH7	PPPSH8	PPPSH9	PPPSH10	PPPSH11
P_n	6.6	7.5	8.1	16.2	17.4	23.0	29.8	32.1	36.3	52.2	68.3
L_K/nm[a]	5.7	6.5	7.0	13.9	15.0	19.8	25.6	27.6	31.2	44.9	58.7
Blend properties											
$PPPS^-/P(EA\text{-}co\text{-}4VPH^+)$											
T_g/°C[b]	1	4	2	4	5	6	4	6	5	3	5
E_Y/MPa	252	263	282	294	318	324	352	367	365	364	349
$PPPS^-/P(S\text{-}co\text{-}4VPH^+)$											
T_g/°C[b]	114	116	115	–[c]	113	114	115	–[c]	–[c]	–[c]	113
E_Y/MPa	55	82	89	114	72	109	86	–[c]	–[c]	–[c]	115

[a] Calculated from $L_K = P_n l_{r.u.}$ with length of repeat unit $l_{r.u.} = 0.86$ nm [42].
[b] As obtained by DSC, second heating run; T_g (P(EA-*co*-4VP)) = −7 °C; T_g (P(S-*co*-4VP)) = 106 °C.
[c] Not measured.

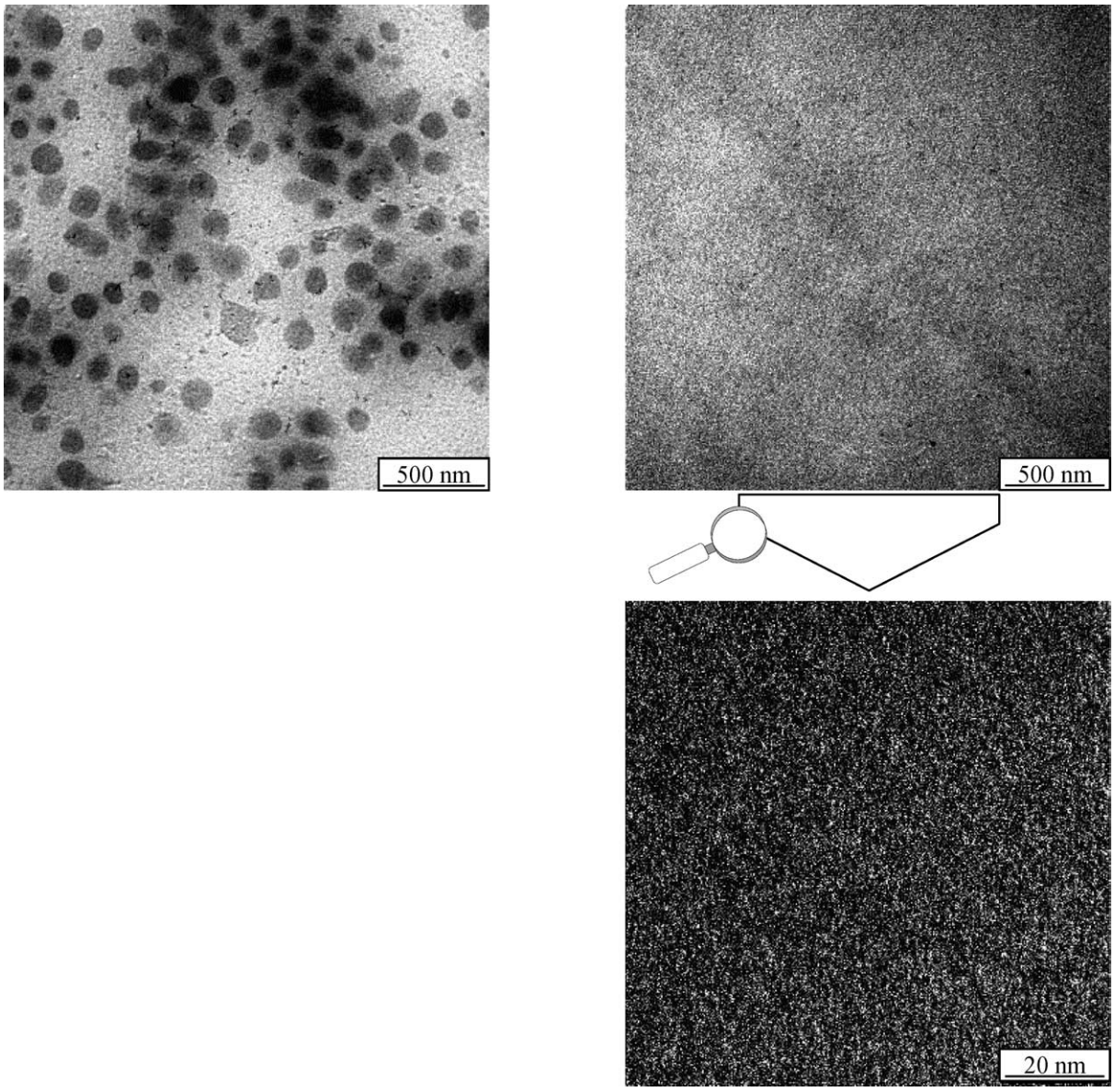

Fig. 7. Transmission electron micrographs (elastic bright field) of blends of *p*-phenylene polymers (Fig. 2) with poly(ethyl acrylate-*co*-4-vinyl pyridine) P(EA-*co*-4VP); (a) phase-separated mixture of the ester precursor polymer PPPSE of the reinforcer (PPPSE 7, Table 1 and Fig. 2) and P(EA-*co*-4VP) without any ionic interactions (28.7 wt% PPPSE), magnification 4000×; (b) ionomer blend PPPS7$^-$/P(EA-*co*-4VPH$^+$) of the poly(*p*-phenylene sulfonic acid) PPPSH 7 and P(EA-*co*-4VP) with attractive interactions (stoichiometry of PPPSH sulfonic and P(EA-*co*-4VP) pyridyl groups), magnification 4000×; (c) same as (b), magnification 125,000×.

molecule: the polyanion characteristics of the rods has been evidenced from the IR-spectra and is to be compensated by matrix counter ions; the implication of this counter ion condensation is discussed further below in the context of the mechanical properties.

High resolution transmission electron microscopy also revealed the molecular miscibility of the rod and coil molecules in the acid/base ionomer blends and confirmed the IR-spectroscopical and DSC results. The TEM micrograph represented in Fig. 7(a) shows the phase-separated morphology of the blend formed from the ester precursor polymer PPPSE and P(EA-*co*-4VP), whereas Fig. 7(b) and (c) show the TEM picture of the single phase PPPS$^-$/P(EA-*co*-4VPH$^+$) ionomer blend. The domains in Fig. 7(a) represent segregated PPPSE microphases. In contrast to this, the high resolution bright field images of the acid/base ionomer blend give no indication whatsoever for heterogeneity. This again is clear proof for the complete miscibility due to the formation of ionic (acid/base) interactions between the PPPSH and P(EA-*co*-4VP) blend components which is not possible in the (phase-separated) blend with PPPSE.

3.2. Mechanical properties and composite model

The special material properties, i.e. the enormous

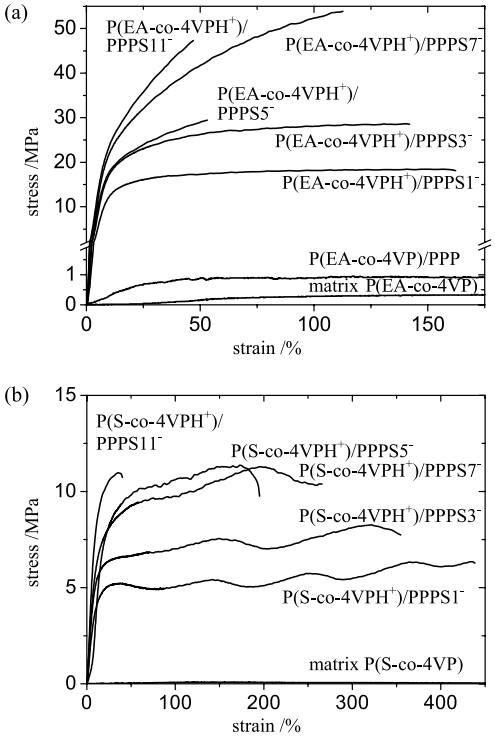

Fig. 8. Stress–strain curves of the matrix polymer and of acid/base ionomer blends with sulfonated poly(*p*-phenylenes) PPPSH of different degrees of polymerization P_n (Table 1). (a) Poly(ethyl acrylate-*co*-4-vinyl pyridine) matrix polymer P(EA-*co*-4VP) and $PPPS^-$/P(EA-*co*-4VPH^+) ionomer blends at room temperature (i.e. about 20–25 K above T_g, Fig. 5); 25 wt% PPPSH and stoichiometry of acid/base groups. (b) Poly(styrene-*co*-4-vinyl pyridine) matrix polymer P(S-*co*-4VP) and $PPPS^-$/P(S-*co*-4VPH^+) ionomer blends at 150 °C (i.e. about 35–40 K above T_g); 23 wt% PPPSH and stoichiometry of acid/base groups.

improvement of the mechanical strength of the acid/base ionomer blends is shown in the stress–strain curves Fig. 8. The pure P(EA-*co*-4VP) matrix polymer is characterized by a Young's modulus of only 0.3 MPa. A modulus increase to about 4 MPa is obtained from the microphase separated blend of P(EA-*co*-4VP) with PPP. Thus, in the PPP/P(EA-*co*-4VP) system which is free of ionic interactions, the PPP phase acts like a filler and the reinforcing effect is moderate. Contrary to this phase-separated system, the molecularly mixed P(EA-*co*-4VPH^+)/$PPPS^-$ blends exhibit much higher moduli ranging from 251 up to 367 MPa (Fig. 8(a)). This translates to reinforcement factors of around 800–1200 related to the pure P(EA-*co*-4VP) matrix or around 60–90 if related to the microphase-separated system PPP/P(EA-*co*-4VP).

Phenomenologically similar results have been obtained for the blends with the P(S-*co*-4VP) matrix (Fig. 8(b)); the modulus increase and the reinforcement factors are somewhat lower which is plausible considering that the measurements have been carried out at a higher temperature relative to T_g (Table 1). In this context, it has to be pointed out that all stress–strain measurements have been carried out well above T_g. Stress–strain data of glassy samples could not be obtained because the ionomer blends turned out to be too brittle as to allow measurements in the glassy state.

As it was to be expected, the reinforcing factor increases with increasing P_n of the rod-like $PPPS^-$ reinforcer, i.e. with increasing aspect ratio [2]. But this (almost linear) increase is only observed within a certain P_n-range (Fig. 9). The data infer that there is a limiting upper value of the reinforcement which does not further increase with increasing P_n of the reinforcers; the beginning of the deviation from the linear relationship corresponds to the exceeding of the persistence length of the poly(*p*-phenylene) molecule which is about 13–25 nm according to literature [27,30].

The measured Young's moduli are significantly higher as expected based on conventional fiber reinforcement effects. It is common pratice to employ the Halpin–Tsai equation (Eq. (1)) [1] for fiber reinforced composites where the fibers form a quasi-isotropic system in a continous matrix.

$$\frac{E}{E_m} = \frac{3}{8}\frac{1+(2L/d)n_L v_f}{1-n_L v_f} + \frac{5}{8}\frac{1+2n_T v_f}{1-n_T v_f} \quad (1)$$

with

$$n_L = \frac{(E_f/E_m)-1}{(E_f/E_m)+2L/d}$$

$$n_T = \frac{(E_f/E_m)-1}{(E_f/E_m)+2}$$

E_m, E_f, modulus of matrix and reinforcer compound; L/d, aspect ratio of reinforcer component; v_f, volume fraction of reinforcer.

Since, the Halpin–Tsai equations were also successfully applied to semi-crystalline polymers with anisotropically arranged crystallites [2], it was obvious to try to treat the rod/coil ionomer blends in a similar manner, especially as

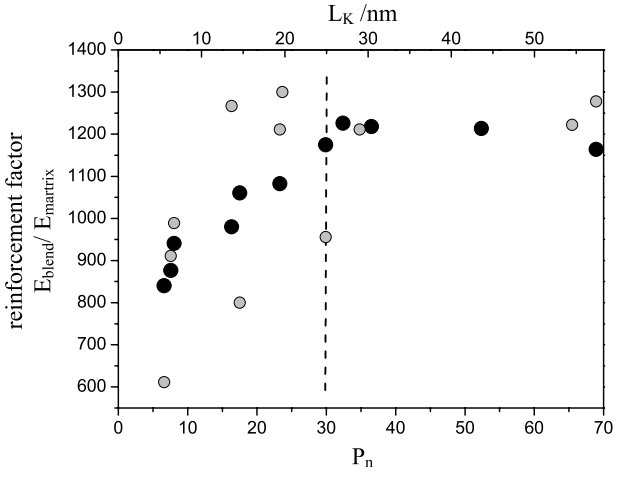

Fig. 9. Dependency of the reinforcement factor (ratio of the experimentally obtained Young's moduli of the blend and of the matrix, [2]) of the acid/base ionomer blends on the degree of polymerization P_n and contour length L_K of PPPSH; (●): $PPPS^-$/P(EA-*co*-4VPH^+) (◍): $PPPS^-$/P(S-*co*-4VPH^+).

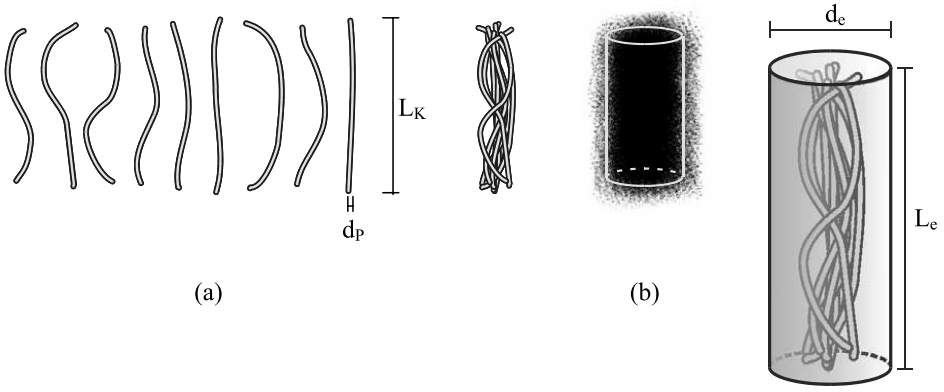

Fig. 10. Illustrative development of the fuzzy cylinder model of worm-like polymer chains: (a) different conformations of the worm-like chain of contour length L_K and chain diameter d_P; (b) visualization of the fuzzy cylinder of length L_e and diameter d_e as given by the spacial overlaying of the conformational fluctuation [34].

they tend to form discontinuous anisotropic phases as well [31,32]. On these lines, reinforcement factors of about 2–35 with an approximately linear relationship between the modulus and aspect ratio of the filler are calculated for, e.g. the $PPPS^-$/P(EA-*co*-4VPH^+) blends. This estimate is based on the assumption that the aspect ratio *L/d* of the rod-like molecules is defined by the PPPSH contour length L_K (varying between 5.7 and 58.7 nm, Fig. 9), and a molecular diameter d_P given either by the polyarylene backbone alone (0.4 nm) or including the alkyl side chains in the extended zig-zag conformation (3.4 nm). As to the other quantities in Eq. (1), the modulus of the matrix $E_m = 0.3$ MPa is the experimentally obtained value; the modulus of the reinforcer PPPSH $E_f = E_{PPPSH} = 360$ GPa is estimated according to Ref. [33], and the volume fraction of the reinforcer $v_f = 0.25$ is the PPPSH weight fraction.

The distinct differences between the experimental and calculated reinforcement factors are attributed to particular molecular interactions and will be interpreted further below. One possibility to explain the deviation of the experimentally determined reinforcement factor from the linear relationship on the rod aspect ratio as resulted from the above procedure is to describe the shape of the reinforcer molecule dispersed in the coiled polymer matrix not like a molecular rigid rod but by the fuzzy cylinder model. This model has been introduced to characterize the rotational diffusion of worm-like chains in solution [34,35]. The length L_e and diameter d_e of the fuzzy cylinder describe the statistical mean volume occupied by the conformational dynamics of the worm-like chains (Fig. 10, [34,36]). In the fuzzy cylinder model, the cylinder height L_e is given by the end-to-end distance of the Kratky–Porod worm-like chain [37]; as long as the chain length of the reinforcer molecules is shorter than its persistence length l_P, the dimensions of the fuzzy cylinder are almost identical to the contour length L_K and diameter d_P of the reinforcer polymer.

The diameter d_e significantly depends on the assumed diameter d_P of the worm-like chain [34]. Given the molecular structure of PPPSH and considering its function in the blend as a molecular reinforcer component, the lower limit of $d_P = 0.4$ nm may be represented by the backbone of the poly(*p*-phenylenes) (Fig. 11(a)), and the upper limit might be given by considering the alkyl side chains in a coiled (Fig. 11(b), $d_P = 2.4$ nm) or even extended all-*trans* conformation (Fig. 11(c), $d_P = 3.4$ nm) in an arrangement perpendicular to the poly(*p*-phenylene) backbone (virtual rod model [25]).

Although the fully extended conformation of the side

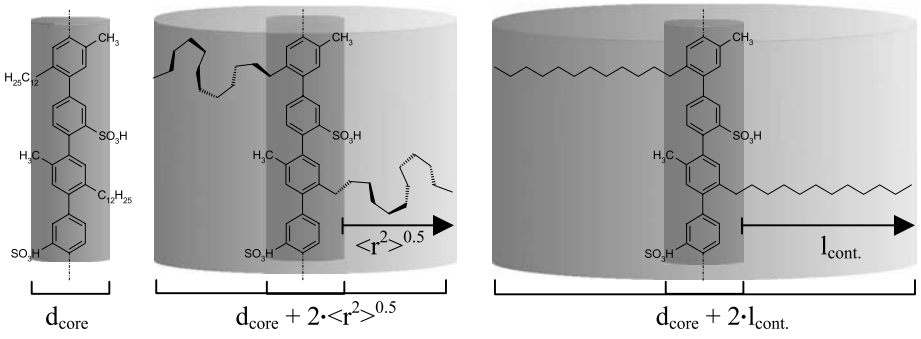

Fig. 11. Illustration of different models to describe the reinforcer relevant diameter d_P of the PPPSH polymer in the ionomer blends: considering the van der Waals diameter of the backbone $d_{core} = 0.4$ nm alone (a), and contribution of the alkyl side chains in the regularly coiled ($\langle r^2\rangle^{0.5} = C_{12}\cdot N\cdot L^2 = 1$ nm [43]) conformation giving $d_P = 2.4$ nm (b), or in the extended zig-zag conformation giving $d_P = 3.4$ nm.

chains is unlikely to occur in the blends, such an effective chain thickness is a constitutionally related clue about the extension of the matrix sphere around the poly(*p*-phenylene) core that may be 'filler-active'. An active contribution of the matrix to the filler volume is reasonable to assume considering the high charge density of the polyelectrolyte reinforcers and the necessary compensation by the vincinity of the counterions. Since, these counterions are bonded to the matrix polymer, matrix elements around the molecular reinforcer are immobilized and, therefore, must be taken into account for the reinforcer volume fraction.

In analogy to the well known phenomenon of 'counterion condensation' in polyelectrolyte solution [38], such intimate ion interactions are likely to occur in a similar fashion in the acid/base ionomer blends. Of course, one has to be aware that this is only a qualitative and phenomenological correspondence considering that the blend is a solid of rather low dielectric constants. Besides, an equilibrium state of counterion condensation cannot be realized in the ionomer blend because the acid–base ionomer formation goes along with a sol–gel transition; this means an effective restriction in the diffusibility of chain segments which impedes further counterion condensation once the network is formed. However, as a net effect of the dynamically incomplete counterion condensation, an effective diameter of the worm-like $PPPS^-$ blend component of 3–4 nm seems to be justified considering the partial immobilization of matrix elements.

The change of the aspect ratio of the PPPSH fuzzy cylinder with the contour length L_K (or degree of polymerization P_n) is shown in curve 3 of Fig. 12. This curve results from the ratio of the end-to-end distance $\langle R^2\rangle^{0.5}$ of a Kratky–Porod worm-like chain (which is the height L_e of the fuzzy cylinder, Fig. 10) and the diameter d_e of the fuzzy cylinder as calculated for a given contour length; the above rationalized $d_P = 3.4$ nm has been considered in the calculation of d_e. The comparison of the shape of the resulting dependency of the aspect ratio from the contour length (curve 3, Fig. 12) with the principle variation of the experimentally determined moduli with the reinforcer molecule length (expressed by P_n) as presented in Fig. 9 infers that it is meaningful to use the fuzzy cylinder model.

This is supported from the relation between the experimentally obtained Young's moduli of the $PPPS^-$/P(EA-*co*-4VPH^+) blends and the calculated aspect ratio of the fuzzy cylinder of the PPPSH molecules of contour length L_K (Fig. 13). The modulus increases linearly with the fuzzy cylinder aspect ratio over the whole aspect ratio range where the upper end includes PPPSH molecules of P_n corresponding two to three times the persistence length l_P.

The multiple attaching of the coiled matrix molecules to the reinforcer via cationic/anionic interactions (i.e. ion condensation) may also be used to explain the high reinforcement factor which is by far beyond the reinforcement values calculated by the conventional Halpin–Tsai equation [39]. It is plausible that the rigid-rod molecules—in addition to their reinforcing effect—also function as a multifunctional, one-dimensional crosslinking agents. The resulting dense network topology is thought to significantly effect the mechanical properties of the ionomer blends.

In this regard, the increase of the tensile strength of the ionomer blend with increasing length (degree of polymerization) of the reinforcing polymer, and also the strain at break which tends to decrease with increasing reinforcer chain length (Fig. 8) give evidence for both topological and dynamic network effects. Since, the total number of ionic groups is constant in all ionomer blends investigated (constant weight fraction of the reinforcing polymer and stoichiometry of acid and base

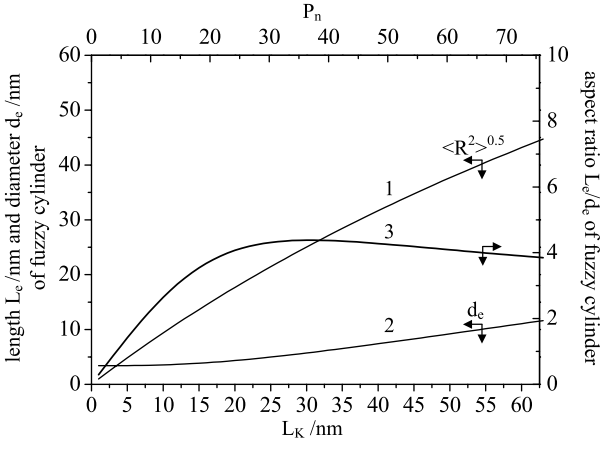

Fig. 12. Dependency of the Kratky–Porod mean square end-to-end distance $\langle R^2\rangle^{0.5}$ ($=L_e$ in Fig. 10) of the worm-like PPPSH (for $l_P = 25$ nm [30]) on the contour length L_K (curve 1), of the dependency of the diameter d_e of the fuzzy cylinder (Fig. 10) for $d_P = 3.4$ nm (Fig. 11) on L_K (curve 2), and the variation of the resulting aspect ratio L_e/d_e of the PPPSH fuzzy cylinder (curve 3).

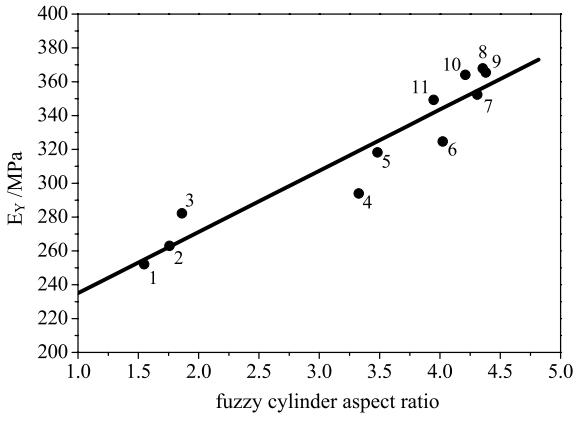

Fig. 13. Correlation of experimentally obtained Young's modulus E_Y of the acid/base ionomer blends $PPPS^-$/P(EA-*co*-4VPH^+) with the calculated theoretical values of the aspect ratio of the PPPSH filler based on the fuzzy cylinder model; PPPSH-parameters used for calculation: contour length L_K as given by the average degree of polymerization P_n (numbers in Fig. 13 referred to abbreviations of sample names in Table 1), persistence length $l_P = 25$ nm [30], and diameter $d_P = 3.4$ nm.

groups), the total number of crosslinking components decreases with increasing degree of polymerization, whereas the functionality of the crosslinking molecules increases at the same time. This means that the network topology changes systematically with increasing PPPSH length; this feature and its relation to rubber elasticity (e.g. Ref. [40]) will be further elucidated in ongoing studies. The yielding behavior in the high-strain range is also reminescent to rubber-based ionomers [41]: similar as in these ionomers, the high values of ultimate elongation observed in the rigid-rod/random-coil ionomer blends may also be associated with ion pair exchanges (ion hopping). This view is in agreement with morphological anisotropies observed in the elongated acid/base ionomer blends.

4. Conclusion

The model studies have shown that molecular reinforcement in polymer materials can be achieved by mixing rod-like molecules with coil molecules provided that sufficiently strong, e.g. ionic interactions are formed between the blend components. The mechanical properties of these ionomeric nanocomposites depend strongly on the molecular parameters of the rod polymer component, i.e. the degree of polymerization P_n, the characteristics of the ionic interactions, and, of course, on the rod volume fraction. The unexpectedly high reinforcement factor is attributed to the pecularities of this molecular polymer/polymer composite as compared to conventional fiber composites: the multiple intermolecular ionic interactions mean a maximized filler-matrix interaction, i.e. both the composite and the network feature of these rigid-rod/random-coil ionomer blends contribute to the outstanding mechanical properties.

The dependency of the mechanical behavior of the blends on the aspect ratio of the molecular filler has been shown to be qualitatively represented by applying the fuzzy cylinder model to describe the size and shape of the reinforcer molecules. However, further studies are needed to comprehensively understand the mutual interrelations in these polyelectrolyte blends, especially as far as the temporary matrix counter-ion distribution along the multiple charged rod polymers is concerned which seems to significantly affect the material properties.

Acknowledgements

The authors would like to thank Dr. R. Thomann (Macromol. Chem., Univ. Freiberg) for the electron microscopy studies. Financial support of part of this work by the Deutsche Forschungsgemeinschaft (Grant No. EI 147/31-1) and the Fonds der Chemischen Industrie is gratefully acknowledged.

References

[1] Kardos JL, Raisoni J. Polym Eng Sci 1975;15:183.
[2] Halpin JC, Kardos JL. Polym Eng Sci 1976;16:344.
[3] Hwang WF, Wiff DR, Benner CL, Helminiak TE. J Macromol Sci Phys 1983;B22:231.
[4] Takayanagi M, Ogata T, Morikawa M, Kai T. J Macromol Sci Phys 1980;B17:591.
[5] Flory PJ. Macromolecules 1978;11:1138.
[6] Li L, Chan CM, Weng LT, Xiang ML, Jiang M. Macromolecules 1998;31:7248.
[7] de Meftahi MV, Frechet JMJ. Polymer 1988;29:477.
[8] Radzilowski LH, Stupp SI. Macromolecules 1994;27:7747.
[9] Zhang L, Huo F, Wang Z, Wu L, Zhang X, Hõppener S. Langmuir 2000;16:3813.
[10] Dormidontova E, Brine G. Macromolecules 1998;31:2110.
[11] Robeson L, McGrath JJ. Polym Eng Sci 1977;17:300.
[12] Pierce E, Kwai T, Min B. J Macromol Sci Chem 1984;A21:1181.
[13] Rochigues-Prada JM, Persec V. Macromolecules 1986;19:55.
[14] Eisenberg A, Smith P, Zhou ZL. Polym Eng Sci 1982;22:1117.
[15] Hara M, Parker GJ. Polymer 1992;33:4685.
[16] Weiss RA, Shao L, Lundberg RD. Macromolecules 1992;25:6370.
[17] Eisenbach CD, Hofmann J, Fischer K. Macromol Chem Rapid Commun 1994;15:117.
[18] Eisenbach CD, Hofmann J, MacKnight WJ. Macromolecules 1994; 27:3162.
[19] Eisenbach CD, Fischer K, Hofmann J. Polym Prepr, Am Chem Soc Div Polym Chem 1995;36/1:795.
[20] Eisenbach CD, Datko A, Göldel A, Hofmann J, Lehmann T, Winter D. Polym Prepr, Am Chem Soc Div Polym Chem 1998;39/1:715.
[21] Eisenbach CD, Fischer K, Hofmann J, MacKnight WJ. Macromol Symp 1999;100:105.
[22] Winter D, Eisenbach CD. J Polym Sci, Part A: Polym Chem 2004;42: 1919.
[23] Winter D, Eisenbach CD. Polymer 2004;45:2507.
[24] Winter D, Eisenbach CD, Pople JA, Gast AP. Macromolecules 2001; 34:5943.
[25] Eisenbach CD, Hofmann J, Göldel A, Noolandi J, Shi AC. Macromolecules 1999;32:1463.
[26] Rulkens R, Schulze M, Wegner G. Macromol Chem Rapid Commun 1994;15:669.
[27] Vanhee S, Rulkens R, Lehmann U, Rosenauer C, Schulze M, Köhler W, Wegner G. Macromolecules 1996;29:5136.
[28] Datko A, Lehmann T, Eisenbach CD. Submitted for publication.
[29] Sakurai K, Douglas EP, MacKnight WJ. Macromolecules 1992;25: 4506.
[30] Petekidis G, Vlassopoulos D, Fytas G, Rulkens R, Wegner G, Fleischer G. Macromolecules 1998;31:6139.
[31] Datko A. Dissertation. Universität Stuttgart; 2000.
[32] Datko A, Eisenbach CD. In preparation.
[33] Wendling J, Wendorff JH. Macromol Theory Simul 1996;5:381.
[34] Sato T, Takada Y, Teramoto A. Macromolecules 1994;24:6220.
[35] Sato T, Teramoto A. Adv Polym Sci 1996;126:85.
[36] Hoshikawa H, Saitô N, Nagayama K. Polym J 1975;7:79.
[37] Kratky O, Porod G. Recl Trav Chim Pays-Bas 1949;68:1106.
[38] Manning G. Ann Rev Phys Chem 1972;23:117.
[39] Bayer A, Datko A, Winter D, Eisenbach CD. Submitted for publication.
[40] Tang M-Y, Mark JE. Macromolecules 1984;17:2616.
[41] Kroschwitz JI, editor. Encyclopedia of polymer science and engineering, vol. 6. Hoboken: Wiley; 2003.
[42] Rulkens R, Wegner G, Enkelmann V, Schulze M. Ber Bunsen-Ges Phys Chem 1996;100:707.
[43] Flory PJ. Statistical mechanics of chain molecules. New York, USA: Interscience; 1969.